A Cyclotomic-Linked Kinematic Model for Continuum Robots and Its Application in Rigid-Flexible Hybrid Arms

Xu Zhang, Shangkui Yang, Peikang Yuan, Zhibin Song, Tao Sun, David T. Branson and Rongjie Kang

Abstract— **The control of continuum robots is generally based on a kinematic model consisting of the actuation-configuration-task spaces. The nonlinear relationship between the actuation and configuration space makes it challenging to build control systems for continuum robots. This paper introduces the cyclotomic-linked kinematic model (CLKM), a pragmatic modeling approach designed to bridge this integration gap by replacing the configuration space with an intuitive joint space. The cornerstone of CLKM is the establishment of a linear relationship between the actuation space and the joint space, which crucially enables the direct application of standard robotic software stacks like ROS, MoveIt, and KDL for control and motion planning. In addition, the CLKM allows a uniform control architecture for continuum modules by using rigid joints, which makes it easy to model the kinematics of rigid-flexible hybrid arms. To validate this approach, a CLKM-based control system of a rigid-flexible hybrid arm prototype is constructed, which mainly utilizes software packages that have been widely used on discrete-jointed robots. The system seamlessly leverages off-the-shelf motion planners from the ROS ecosystem, and experimental results in path tracking tasks demonstrate its practical effectiveness, achieving a maximum tracking error below 1.5% of the continuum module's length.**

I. Introduction

Continuum robots have been focused on by researchers in the field of robotics due to their inherent compliance and hyper-redundant nature [1]–[3]. Unlike traditional discrete joints, continuum-type joints (i.e., continuum modules) do not have fixed axes of motion, and their motion is formed by bending of the arm's backbone. This distinction forms the basis of both their unique capabilities and the primary challenges in their control [4], [5].

To accurately describe the unique bending freedoms of continuum modules for control purposes, researchers have done a lot of work on the kinematic modeling for continuum robots [6], [7]. Walker et al. proposed the configuration space to describe the shape of continuum robots and designed a kinematic model structure of actuation-configuration-task spaces, which greatly extended the controllability of continuum robots [8], [9].

Based on the configuration space, other researchers have carried out extensive work to optimize the performance of kinematic models for continuum robots. For example, using continuum mechanics principles such as Cosserat, Kirchhoff, and Euler-Bernoulli rod/beam theories to describe configuration changes in order to improve the accuracy of kinematic models [10]–[14]. It is also possible to build a reduced-order kinematic model (ROM) based on the principles of mechanics and geometry. These models used piecewise constant curvature (PCC), cubic spline and Bezier spline, etc. to describe the configuration space, reducing the complexity of the kinematics and increasing the speed of the computation [4], [15], [16].

However, these works have mainly focused on the relationship between the configuration space and the task space, while neglecting the relationship between the actuation space and the configuration space. Compared to the joint space of traditional discrete-jointed robots, the configuration space of continuum robots has a significant difference. That is the physical connection between the actuation space and the joint space of discrete-jointed robot is simply a set of reducers with fixed reduction ratios, allowing a linear relationship. However, the configuration space of continuum modules is a set of parameters describing their shape curves and has a non-linear relationship with the actuation space (i.e., the length of the driving cables) [17], [18]. This nonlinearity creates a fundamental "integration gap" with the vast ecosystem of highly-optimized software developed for traditional discrete-jointed robots. Frameworks like ROS and MoveIt, which are standard in robotics research and application, are architected around the concept of a joint space with well-defined, often linear or easily invertible relationships [19]. Consequently, applying these powerful tools to continuum robots is not straightforward. Researchers are often forced to either develop custom control and planning algorithms from scratch—effectively "reinventing the wheel" [20]. Moreover, for some continuum robots, obtaining the explicit inverse solution of the kinematics between actuation space and configuration space is difficult [5]. Researchers had to employ an additional numerical iteration step to solve this problem, which greatly increased the complexity of the control system. This barrier significantly hinders the rapid prototyping, deployment, and adoption of continuum robots in more complex, real-world applications [21], [22].

To address this challenge, this paper proposes the cyclotomic-linked kinematic model (CLKM) to approximate a continuum module to a series of equal length links located on its secants. As a result, the bending motion of the continuum

* This work was supported by the Natural Science Foundation of China (Grant No. 52375023). (Corresponding author: Rongjie Kang.)

Xu Zhang is with the Key Laboratory of Mechanism Theory and Equipment Design of Ministry of Education, School of Mechanical Engineering, Tianjin University, Tianjin 300072, China. (e-mail: tju_zhangxu@tju.edu.cn).

David T. Branson is with the Advanced Manufacturing Technology Research Group, Faculty of Engineering, University of Nottingham, NG7 2RD Nottingham, U.K. (e-mail: david.branson@nottingham.ac.uk).

Shangkui Yang, Peikang Yuan, Zhibin Song, Tao Sun and Rongjie Kang are with the Key Laboratory of Mechanism Theory and Equipment Design of Ministry of Education, School of Mechanical Engineering, Tianjin University, Tianjin 300072, China (e-mail: yangshangkui@tju.edu.cn, yuanpeikang@tju.edu.cn; songzhibin@tju.edu.cn; stao@tju.edu.cn; rjkang@tju.edu.cn).

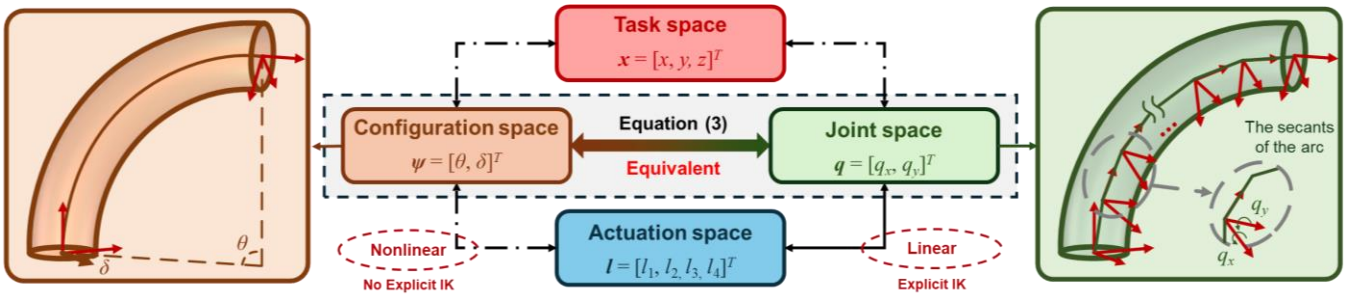

Figure 1. The cyclotomic-linked kinematic model of continuum robot.

module is equivalent to a series of coupled discrete rotational motions. Instead of pursuing higher modeling fidelity, the core philosophy of CLKM is to establish a direct, linear relationship between the actuation space and the defined joint space. This modeling approach allows the continuum module to be treated conceptually as a standard serial chain of virtual joints, making it directly compatible with existing control and planning robotic infrastructures.

The paper is organized as follows: the cyclotomic-linked kinematic model (CLKM) of a continuum robot is established in Section 2. The structure and kinematics of the rigid-flexible hybrid arm are presented in Section 3. Section 4 validates the presented control system based on the CLKM through experiments. Conclusions are eventually given in Section 5.

II. The Cyclotomic-Linked Kinematic Model

In this section, a cyclotomic-linked kinematic model (CLKM) for continuum robots is proposed, and the linear correlation between the actuation space and joint space in the CLKM is demonstrated. In addition, the equivalence between the CLKM and the constant-curvature kinematic model (CCKM) [9] is analyzed.

A. The cyclotomic-linked kinematic model

The proposed CLKM is a geometric approximation designed to simplify the kinematics of continuum robots. The fundamental concept is to discretize the continuous backbone of a module into a series of n rigid links of equal length, connected by virtual rotational joints. As shown in Fig. 1, each continuum module is considered as a series of equal secants on an arc of constant curvature, and each secant is a link in the CLKM. Due to the same length of the secants, the angle between the neighboring links is equal. And the bending motion of the continuum module is considered as the coupled rotational joints between the links. As a result, the configuration space of the CCKM is replaced with the joint space of the CLKM. A continuum module in the CLKM can be represented as three spaces: the actuation space, the joint space and the task space.

The actuation space is described by the length of each driving cables l_i (i is the index of driving cables, and i = 1,2,3, 4 in this paper). The joint space is described by the angles of the two rotational joints in series between two neighboring links $q_{j,x}$, $q_{j,y}$ (j is the index of joints, and $j_{max} = n$, where n is the number of the links). In detail, the two links contain two rotational joints along the x, y directions, respectively. The rotation matrix of the joint in the CLKM is

$$\begin{aligned}\boldsymbol{R}_j &= Roty(q_{j,y}) \bullet Rotx(q_{j,x}) \\ &= \begin{bmatrix} \cos(q_{j,y}) & 0 & \sin(q_{j,y}) \\ 0 & 1 & 0 \\ -\sin(q_{j,y}) & 0 & \cos(q_{j,y}) \end{bmatrix} \begin{bmatrix} 1 & 0 & 0 \\ 0 & \cos(q_{j,x}) & -\sin(q_{j,x}) \\ 0 & \sin(q_{j,x}) & \cos(q_{j,x}) \end{bmatrix}\end{aligned} \tag{1}$$

It is in fact a decomposition of the bending degrees of freedom in the CCKM into two orthogonal planes. Thus, $q_{j,x}$, $q_{j,y}$ of the CLKM can be considered to be related to the configuration angle in the CCKM as:

$$\begin{cases} \sum_{j=0}^{n} q_{j,x} = -\theta \cdot \sin\delta = q_x \\ \sum_{j=0}^{n} q_{j,y} = \theta \cdot \cos\delta = q_y \end{cases} \tag{2}$$

where θ is the center angle of the arc in the CCKM, δ is the angle between the bending plane and the x-z plane [19]. In addition, from the geometric relationship of the secants it can be obtained that

$$\begin{cases} q_{j,x(y)} = \dfrac{1}{2n} q_{x(y)}, j = 0, n \\ q_{j,x(y)} = \dfrac{1}{n} q_{x(y)}, j = 1, 2, ..., n-1 \end{cases} \tag{3}$$

The task space is described as the position of end-tip $\boldsymbol{x} = [x, y, z]^{\mathrm{T}}$. According to Equation (1), we can obtain the transformation matrix of each joint as:

$$\boldsymbol{T}_j^{j+1} = \begin{bmatrix} \boldsymbol{R}_j & \boldsymbol{R}_j \boldsymbol{P}_j \\ 0 & 1 \end{bmatrix}, j = 0, 1, ..., n \tag{4}$$

And the vector of translation is

$$\boldsymbol{P}_j = \begin{cases} [0, 0, L/n]^T, j = 0, 1, ..., n-1 \\ [0, 0, 0]^T, j = n \end{cases} \tag{5}$$

where L is the length of the continuum module. So, we can get the transformation matrix of end-tip according to Equation (4) as:

$$\boldsymbol{T} = \boldsymbol{T}_0^1 \boldsymbol{T}_1^2 ... \boldsymbol{T}_n^{n+1} \tag{6}$$

B. Linear correlation between actuation space and joint space

In the CCKM [19], the relationship between the actuation space and the configuration space is

$$l_i = L + r\cos(\delta + (i-1)\frac{\pi}{2})\theta \tag{7}$$

where r is the distribution radius of driving cables.

According to Equation (2) and (7), the relationship between the actuation space and the joint space in the CLKM can be derived as

$$\begin{aligned} l_i &= L + r\cos((i-1)\frac{\pi}{2})\theta\cos\delta - r\sin((i-1)\frac{\pi}{2})\theta\sin\delta \\ &= L + r\cos((i-1)\frac{\pi}{2})q_y + r\sin((i-1)\frac{\pi}{2})q_x \end{aligned} \tag{8}$$

The matrix form can be expressed as

$$\boldsymbol{l} = \begin{bmatrix} l_1 \\ l_2 \\ l_3 \\ l_4 \end{bmatrix} = \begin{bmatrix} L \\ L \\ L \\ L \end{bmatrix} + r\begin{bmatrix} 0 & 1 \\ 1 & 0 \\ 0 & -1 \\ -1 & 0 \end{bmatrix}\boldsymbol{q} \tag{9}$$

where $\boldsymbol{q} = [q_x, q_y]^T$ is the joint space in the CLKM. It can be seen that the relationship between the actuation space and the joint space is completely linearly correlated.

C. Model approximation error and comparison with CCKM

While the CLKM provides a valuable linear mapping, it is essential to quantify the discretization error introduced by this approximation. This error, which arises from modeling a smooth constant-curvature curve with a series of straight-line segments, represents the deviation of the CLKM from the well-established CCKM. The purpose of the following simulation is to analyze this deviation and show that for a sufficient number of links (n), the CLKM serves as a high-fidelity approximation of the CCKM, justifying its use. A set of simulations are carried out to make a comparison between the CLKM and the CCKM. For a continuum module, different joint angles $\boldsymbol{q} = [q_x, q_y]^T$ (the CCKM can be transformed into configuration angles $\boldsymbol{\psi} = [\theta, \delta]^T$ by Equation (2)) are given to compare the error in the task space.

Figure 2 shows the error of CLKM compared to CCKM for different joint angles $\boldsymbol{q}$ and number of the links n (Due to the central symmetry of the kinematics, only the case of $q_x > 0$, $q_y > 0$ is shown here). It can be seen that as the number of links

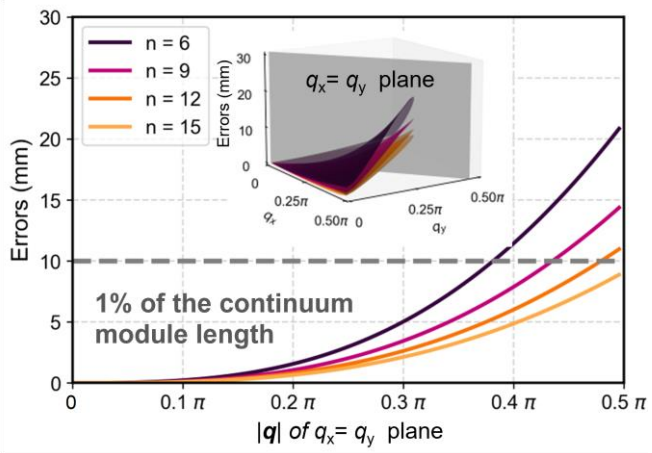

Figure 2. Errors of the CLKM compared to the CCKM for different joint angles $\boldsymbol{q}$ and number of the links n.

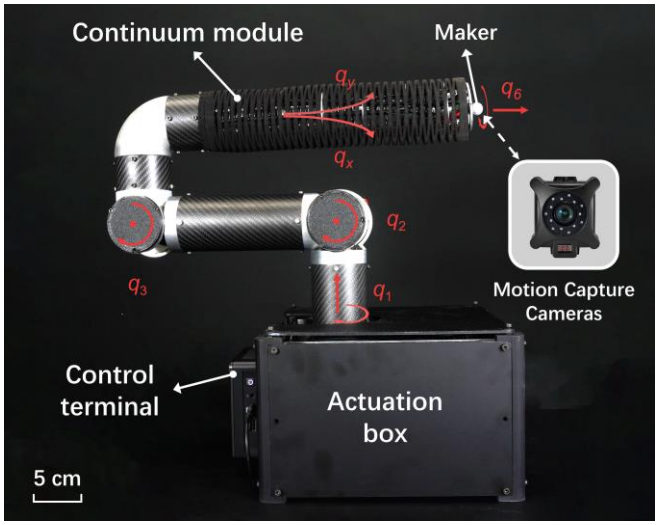

Figure 3. Prototype of the rigid-flexible hybrid arm.

n is larger or the joint angles $\boldsymbol{q}$ is smaller, the error will get smaller. That's because the length of the links in the CLKM is fixed, but the length of the secants in the CCKM will be smaller as the configuration θ (i.e., joint angles $\boldsymbol{q}$) increases. The difference of length between the links and the secents leads to errors. In addition, the difference of length between the links and the secents becomes smaller when n increases, so the errors become smaller as well. However, it can also be seen that the maximum error is less than 1% of the continuum module length when $n \geq 15$, which shows that the CLKM and the CCKM have similar accuracy for continuum robots. A larger n will reduce the computational efficiency, so in this paper $n = 15$.

III. Prototype

To demonstrate the practical viability and integration capability of the CLKM, a prototype of the rigid-flexible hybrid arm containing a continuum module is introduced. Due to the uniform use of joint space in the CLKM, a kinematic model of the arm is established easily. In addition, a control software is constructed which uses proven software resources of traditional discrete-jointed robots.

A. Prototype of the rigid-flexible hybrid arm

Figure 3 shows the prototype of the rigid-flexible hybrid arm with 6 degrees-of-freedom (DOF). The arm is composed of 4 rigid joints and a 2-DOF continuum module. The continuum module contains a super-elastic NiTi alloy backbone (2mm in diameter), four driving cables (0.6mm in diameter) and several constraint disks [23]. The length of the continuum module is 320mm. The four driving cables are divided into two closed-loop sets. Two driving cables of each set with a 180° distribution are connected to the same servo motor in the actuation box. The driving cables are covered by Bowden tubes when pass through the rigid parts of rigid-flexible hybrid arm [24]. All servo motors (HCA-60, Daran Technology Co., Ltd, China) of rigid joints and continuum modules are connected to a NUC minicomputer (Intel Corp., America) through the CAN (Controller Area Network) bus. In addition, an optical motion capture system (NOKOV Inc., China) including several cameras and a marker

is used to collect the experimental data on the position of the arm end-tip for performance evaluation.

B. The kinematic model of the rigid-flexible hybrid arm

A key advantage of the CLKM is its ability to provide a unified kinematic representation for the rigid-flexible entire hybrid arm. By modeling the continuum module as a series of virtual joints, the arm can be modeled using a standard Denavit-Hartenberg (D-H) parameter table, just as one would for a discrete-jointed robots.

TABLE I. D-H PARAMETER TABLE

Link	α_i	a_i	θ_i	d_i
1	0	0	q_1	280
2	π/2	0	$\pi + q_2$	0
3	0	240	$-2\pi/3 + q_3$	0
4	0	187	$-\pi/3$	0
cm_0	π/4	0	$q_x/2n$	0
	$-\pi/2$	L/n	$q_y/2n$	0
cm_1	π/2	0	q_x/n	0
	$-\pi/2$	L/n	q_y/n	0
cm_2	π/2	0	q_x/n	0
	$-\pi/2$	L/n	q_y/n	0
		...		
cm_{n-1}	π/2	0	q_x/n	0
	$-\pi/2$	L/n	q_y/n	0
cm_n	π/2	0	$q_x/2n$	0
	$-\pi/2$	0	$q_y/2n$	0
6	$-\pi/4$	34	q_6	0

As shown in TABLE I. , the continuum module is considered as a series of links cm_0, cm_1, … cm_n based on the CLKM. And there are two series joints between two neighboring links according to Equation (1), thus the $2(n + 1)$ sets of D-H parameters to express the continuum module.

C. Control system

Based on the CLKM, a control system is built on ROS (Robot Operating System) for the rigid-flexible hybrid arm. As shown in Fig. 4, the control system includes four software packages to realize kinematics, motion planning, human-robot interface, and joint controller. The kinematics package is

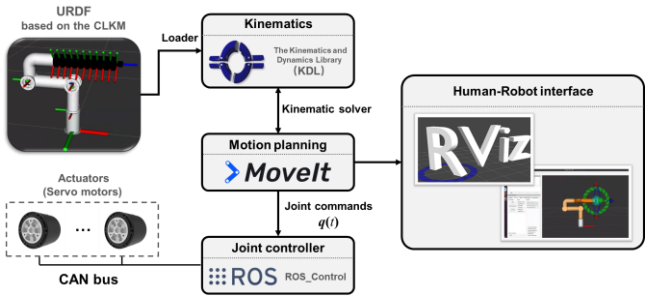

Figure 4. Control system of the rigid-flexible hybrid arm

based on the kinematics and dynamics library (KDL), which can load URDF (Unified Robot Description Format) files and build the forward and inverse kinematics solvers. Due to the application of the joint space in the CLKM, the kinematics of the rigid-flexible hybrid arm can be formulated into a topological network of the joints and links, i.e., an URDF file. The motion planning package is MoveIt integrating multiple motion planning libraries (e.g. The Open Motion Planning Library (OMPL), including PRM, EST, RRT, RRT*,SBL, etc. [25]) and trajectory processing algorithms (e.g. Cubic spline, quintuple spline and straight line). It is a fact that the MoveIt cannot work without the kinematics solver provided by the KDL, which benefits from the use of the joint space in the CLKM. In addition, the MoveIt provides the interface to the RVIZ package, which can be used to operate the rigid-flexible hybrid arm in an interactive Human-Robot interface. Then the MoveIt computes the joint commands $\boldsymbol{q}(t)$ to send to the ROS_Control package.

The ROS_Control is a joint-level PID controller, which establishes a closed-loop control between the actuation space and joint space. Since the ROS_Control is typically applied to rigid discrete-jointed robots whose physical connection between the actuators and the joints is a set of reducers with fixed reduction ratios, it requires that the relationship between the actuation space and joint space be linear. This makes the CCKM with nonlinear mapping between the actuation space and configuration space unavailable to the ROS_Control package. But for the CLKM, the conclusion that it has a linear mapping between the actuation space and joint space has been demonstrated by Equation (9) in Section II-B. In this prototype, the ROS_Control communicates with the actuators

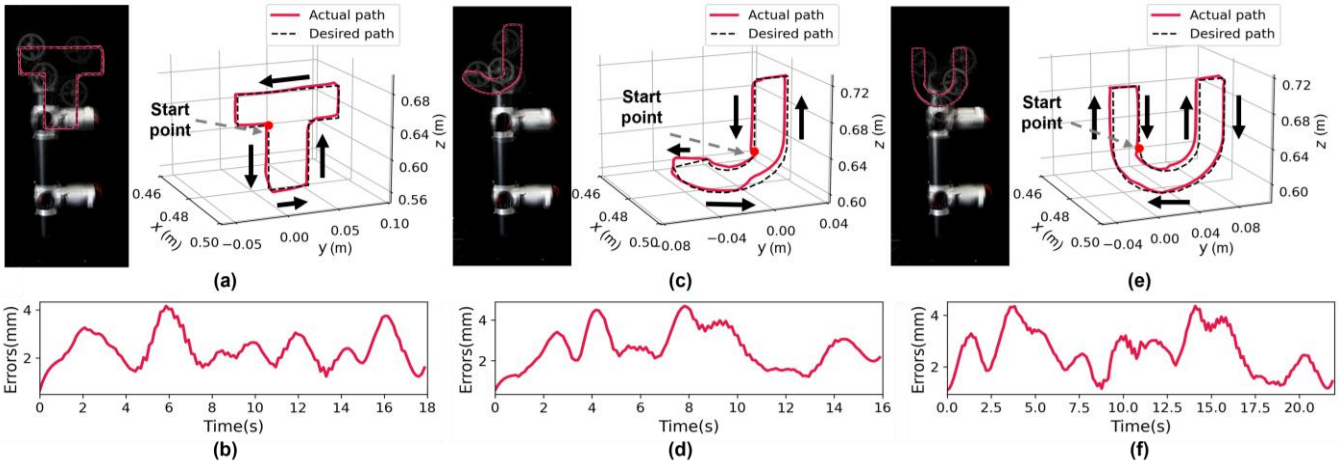

Figure 5. Experimental results of trajectory tracking: (a-b) the letter "T" and the tracking errors, (c-d) the letter "J" and the tracking errors, (e-f) the letter "U" and the tracking errors

(i.e. servo motors) through a CAN Bus.

Due to the use of rich software packages that have been widely used on discrete-jointed robots, the control system development cycle of the rigid-flexible hybrid arm is extremely short. The control system can be constructed by simply writing an URDF file (only 81 lines) to access the software packages and importing the hardware interface, which includes kinematics, motion planning, joint controllers and other functions (The code is available at https://github.com/Prologue-Z/rf_hybrid_arm.). In addition, the control system using mature software packages has some significant advantages such as rich control interfaces and excellent user-friendliness. These advantages help operators develop applications in a more efficient way.

IV. Experiments

To evaluate the practical performance and versatility of the proposed CLKM-based control system, two sets of experiments (path tracking and planning experiments) on the hybrid arm prototype are conducted.

A. Path tracking

The path tracking experiment was designed to quantify the end-tips tracking accuracy of the system. In this experiment, we design a set of discrete points $\{\boldsymbol{x}_1, \boldsymbol{x}_2, \boldsymbol{x}_3 \ldots\}$. Then, the

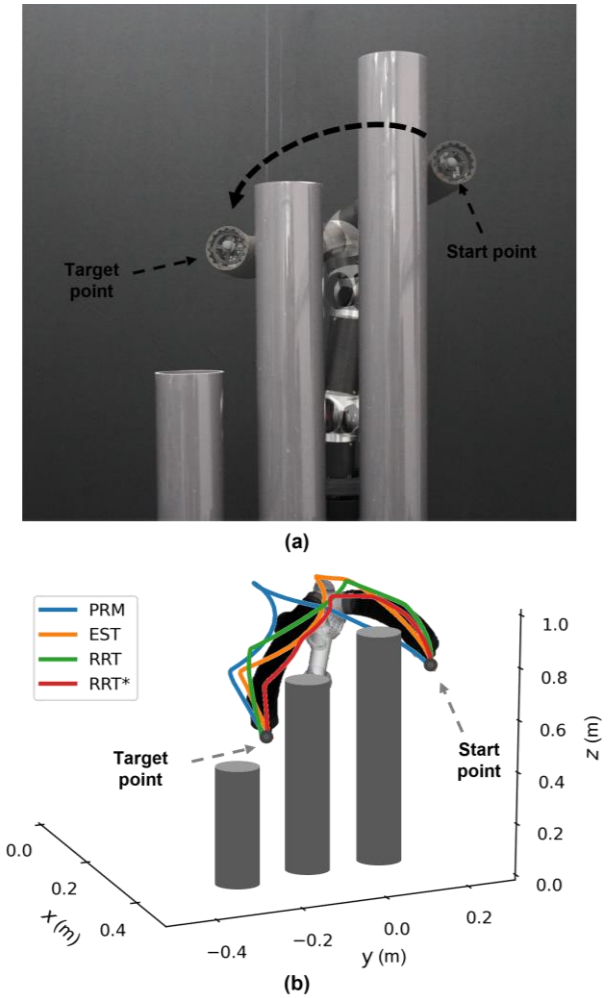

Figure 6. Experimental results of obstacle avoidance with multiple planners: (a) scenario setup, (b) results of planning and execution.

TABLE II. Comparison For Multiple Planners.

Planner	Times (s)	Path length (mm)
PRM	0.28	1213.5
EST	0.37	1082.8
RRT	0.20	1010.4
RRT*	18.80	915.5

trajectory processing (straight line) functions of the MoveIt package are used to process the points into a time-sequenced desired path $\boldsymbol{x}_d(t)$ that can be executed by the rigid-flexible hybrid arm. After that, the inverse kinematics solver provided by KDL converts $\boldsymbol{x}_d(t)$ to a path $\boldsymbol{q}_d(t)$ in the joint space. Finally, the joint controller sends commands to the servo motors.

As shown in Fig. 5, the three sets of desired paths are the three letters "TJU" (abbreviation of Tianjin University). And the experimental results showed that the maximum errors for the three sets of paths are 4.16, 4.36 and 4.68mm respectively. The errors are mainly due to mechanical assembly errors and gravity, and are less than 1.5 % of the length of the continuum module. This experiment shows that the CLKM-based control system has excellent accuracy.

B. Path planning

The path planning experiment aims to showcase the primary advantage of the CLKM: the ability to leverage sophisticated, off-the-shelf motion planners. In this experiment, several obstacles were deployed in the workspace of the rigid-flexible hybrid arm, as shown in Fig. 6(a). The control system needs to use planners to get a path from the start point to target point. Due to the application of CLKM, the rigid-flexible hybrid arm can directly use more than 10 planners in OMPL. And four common planners including PRM, EST, RRT, and RRT* were used to carry out experiments, where RRT* sets the path length as the optimization objective.

As shown in Fig. 6(b), the planners respectively give a path that can pass around the obstacles to reach the target point. Table 2 shows the computation time and path length. RRT* planner uses the maximum computation time 18.8s but got the shortest paths. In comparison, RRT use the minimum computational time of only 0.2s. This experiment shows that the CLKM-based control system is adapted to multiple planners, which makes it easy to develop in different scenarios.

V. Conclusion

This paper introduced the cyclotomic-linked kinematic model (CLKM), a modeling method designed to bridge the integration gap between continuum robots and discrete-jointed robotic software ecosystems. Then the line correlation between the actuation space and the joint space of CLKM was verified. So that the CLKM allows continuum module to be controlled and planned for using standard, off-the-shelf tools.

Next, a prototype of the rigid-flexible hybrid arm containing a continuum module was built. A kinematic model of the arm was established based on the CLKM. And a control system of the rigid-flexible hybrid arm was constructed. The control system mainly used software packages that have been widely used on discrete-jointed robots, i.e. MoveIt, KDL and

ROS_Control. So, the control system can be constructed by simply writing an URDF file (only 81 lines).

Finally, path tracking and planning experiments were carried out based on the CLKM-based control system. In the path tracking experiments, the rigid-flexible hybrid arm moved along the desired path. And the maximum tracking error is less than 1.5% of the length of the continuum module, which shows the excellent accuracy of the CLKM-based control system. In addition, the control system used four planners such as PRM, EST, RRT, and RRT* in OMPL for path planning in a scenario with multiple obstacles. The RRT planner gives a feasible path in only 0.2s and the RRT* gives the shortest path. This demonstrates the easy-to-use and versatility of the CLKM-based control system for different requirements.

ACKNOWLEDGMENT

This work was supported by the National Natural Science Foundation of China (grant no. 52375023).

REFERENCES

[1] C. Armanini, F. Boyer, A. T. Mathew, C. Duriez, and F. Renda, "Soft robots modeling: A structured overview," IEEE Trans. Robot., vol. 39, no. 3, pp. 1–21, 2023.

[2] J. Burgner-Kahrs, D. C. Rucker, and H. Choset, "Continuum robots for medical applications: A survey," IEEE Trans. Robot., vol. 31, no. 6, pp. 1261–1280, 2015.

[3] R. J. Webster and B. A. Jones, "Design and kinematic modeling of constant curvature continuum robots: A review," Int. J. Rob. Res., vol. 29, no. 13, pp. 1661–1683, 2010.

[4] Z. Gong, X. Fang, X. Chen, J. Cheng, Z. Xie, J. Liu, B. Chen, H. Yang, S. Kong, Y. Hao, T. Wang, J. Yu, and L. Wen, "A soft manipulator for efficient delicate grasping in shallow water: Modeling, control, and real-world experiments," Int. J. Rob. Res., vol. 40, no. 1, pp. 449–469, 2021.

[5] X. Zhang, Y. Liu, D. T. Branson, C. Yang, J. S. Dai, and R. Kang, "Variable-gain control for continuum robots based on velocity sensitivity," Mech. Mach. Theory, vol. 168, p. 104618, 2022.

[6] M. Russo, S. M. H. Sadati, X. Dong, A. Mohammad, I. D. Walker, C. Bergeles, K. Xu, and D. A. Axinte, "Continuum robots: An overview," Adv. Intell. Syst., p. 2200367, 2023.

[7] X. Wang, Y. Li, and K.-W. Kwok, "A survey for machine learning-based control of continuum robots," Front. Robot. AI, vol. 8, p. 730330, 2021.

[8] I. A. Gravagne, C. D. Rahn, and I. D. Walker, "Large deflection dynamics and control for planar continuum robots," IEEE/ASME Trans. Mechatron., vol. 8, no. 2, pp. 299–307, 2003.

[9] B. A. Jones and I. D. Walker, "Kinematics for multisection continuum robots," IEEE Trans. Robot., vol. 22, no. 1, pp. 43–55, 2006.

[10] F. Boyer, V. Lebastard, F. Candelier, and F. Renda, "Dynamics of continuum and soft robots: A strain parameterization based approach," IEEE Trans. Robot., vol. 37, no. 3, pp. 847–863, 2021.

[11] F. Renda, M. Giorelli, M. Calisti, M. Cianchetti, and C. Laschi, "Dynamic model of a multibending soft robot arm driven by cables," IEEE Trans. Robot., vol. 30, no. 5, pp. 1109–1122, 2014.

[12] D. C. Rucker and R. J. Webster, "Statics and dynamics of continuum robots with general tendon routing and external loading," IEEE Trans. Robot., vol. 27, no. 6, pp. 1033–1044, 2011.

[13] J. Till, V. Aloi, and C. Rucker, "Real-time dynamics of soft and continuum robots based on cosserat rod models," Int. J. Rob. Res., vol. 38, no. 6, pp. 723–746, 2019.

[14] C. Yang, S. Geng, I. Walker, D. T. Branson, J. Liu, J. S. Dai, and R. Kang, "Geometric constraint-based modeling and analysis of a novel continuum robot with shape memory alloy initiated variable stiffness," Int. J. Rob. Res., vol. 39, no. 14, pp. 1620–1634, 2020.

[15] S. M. H. Sadati, S. E. Naghibi, A. Shiva, B. Michael, L. Renson, M. Howard, C. D. Rucker, K. Althoefer, T. Nanayakkara, S. Zschaler, C. Bergeles, H. Hauser, and I. D. Walker, "TMTDyn: A matlab package for modeling and control of hybrid rigid–continuum robots based on discretized lumped systems and reduced-order models," Int. J. Rob. Res., vol. 40, no. 1, pp. 296–347, 2021.

[16] C. Della Santina, R. K. Katzschmann, A. Bicchi, and D. Rus, "Model-based dynamic feedback control of a planar soft robot: Trajectory tracking and interaction with the environment," Int. J. Rob. Res., vol. 39, no. 4, pp. 490–513, 2020.

[17] Y.-J. Kim, S. Cheng, S. Kim, and K. Iagnemma, "A stiffness-adjustable hyperredundant manipulator using a variable neutral-line mechanism for minimally invasive surgery," IEEE Trans. Robot., vol. 30, no. 2, pp. 382–395, 2014.

[18] M. Li, R. Kang, D. T. Branson, and J. S. Dai, "Model-free control for continuum robots based on an adaptive kalman filter," IEEE/ASME Trans. Mechatron., vol. 23, no. 1, pp. 286–297, 2018.

[19] K. Xu and N. Simaan, "An investigation of the intrinsic force sensing capabilities of continuum robots," IEEE Trans. Robot., vol. 24, no. 3, pp. 576–587, 2008.

[20] C. Wang, S. Geng, D. T. Branson, C. Yang, J. S. Dai, and R. Kang, "Task space-based orientability analysis and optimization of a wire-driven continuum robot," Proc. Inst. Mech. Eng. C. J. Mech. Eng. Sci., vol. 233, no. 23–24, pp. 7658–7668, 2019.

[21] W. Yu, N. Gileadi, C. Fu, S. Kirmani, K.-H. Lee, M. G. Arenas, H.-T. L. Chiang, T. Erez, L. Hasenclever, J. Humplik, B. Ichter, T. Xiao, P. Xu, A. Zeng, T. Zhang, N. Heess, D. Sadigh, J. Tan, Y. Tassa, and F. Xia, "Language to Rewards for Robotic Skill Synthesis." arXiv, Jun. 16, 2023.

[22] Z. Fu, T. Z. Zhao, and C. Finn, "Mobile ALOHA: learning bimanual mobile manipulation with low-cost whole-body teleoperation." arXiv, Jan. 04, 2024.

[23] X. Zhang, C. Yang, Z. Song, M. A. Khanesar, D. T. Branson, J. S. Dai, and R. Kang, "An adaptive lumped-mass dynamic model and its control application for continuum robots," Mech Mach Theory, vol. 201, p. 105736, 2024.

[24] C. Sun, R. Kang, P. Yuan, L. Chang, X. Dong, S. Wan, Z. Song, and J. S. Dai, "Design and modeling of a cable-driven hollow continuum manipulator," in Proceedings of the IEEE International Conference on Advanced Robotics and Mechatronics (ICARM), Sanya, China, Jul. 2023, pp. 55–60.

[25] I. A. Sucan, M. Moll, and L. E. Kavraki, "The open motion planning library," IEEE Robot. Autom. Mag., vol. 19, no. 4, pp. 72–82, 2012.